Available online at www.sciencedirect.com
ScienceDirect
Catalysis Today 128 (2007) 138–144
CATALYSIS TODAY
www.elsevier.com/locate/cattod

Interface science for optimizing the size of oxidic nanoparticles in supported catalysts

K. Bourikas [a], J. Vakros [a], Ch. Fountzoula [a], Ch. Kordulis [a,b], A. Lycourghiotis [a,*]

[a] *Department of Chemistry, University of Patras, GR-265 00, Patras, Greece*
[b] *Institute of Chemical Engineering & High Temperature Chemical Processes, (FORTH/ICE-HT) P.O. Box 1414, GR-265 00, Patras, Greece*

Available online 9 August 2007

Abstract

In the present work we attempt to optimize the size of the supported ''molybdenum oxide''/titania and ''cobalt oxide''/γ-alumina nanoparticles formed after calcination by ''selecting'', respectively, the proper mode of deposition and the local structure of the deposited species achieved upon the impregnation step of catalyst preparation. Concerning the first system, it was found that the disubstituted Mo inner sphere surface complexes, which are bound on the support surface stronger than the monosubstituded ones, resist more effectively to the sintering taking place during calcination where the above complexes are transformed progressively into MoO_3 supported nanoparticles. This leads to a catalyst with very small MoO_3 nanoparticles and thus with very high activity for the selective reduction of NO by NH_3. Concerning the ''cobalt oxide''/γ-alumina catalysts, it was found that a relatively large (small) size of the supported nanocrystallites is imposed by the bulk deposition (formation of inner sphere surface complexes). A quite small size of the supported ''cobalt oxide'' nanocrystallites, not strongly interacted with the support surface, is imposed by the interface precipitation. This is the optimum supported phase for the complete oxidation of benzene.

Keywords: Preparation of supported catalysts; Catalytic activity; Oxidic nanoparticles; Equilibrium deposition filtration (EDF); Incipient wetness impregnation; Interface chemistry; Adsorption; Deposition; Precipitation; Surface complexes; Local structure

1. Introduction

The size of the supported oxidic nanoparticles is frequently a key factor determining catalytic behavior [1]. Obviously, a decrease in this size leads to an increase of the active surface. On the other hand, such a decrease causes an increase in the ''supported particles''/support interactions and thus hinders the reducibility of the supported ions as well as their ability to exchange electrons with the adsorbed reactants. Moreover, such a decrease below a critical value (e.g. 4 nm) may bring about a destruction of the structure of the active sites. This is the case of the structure-sensitive reactions. In contrast, an increase in the size of the supported oxidic nanoparticles brings about a decrease in the active surface and in the above mentioned interactions as well. Too weak interactions allow the surface migration of the supported particles and thus facilitate an additional decrease of the active surface through sintering. In view of the above the optimization of the size of the supported oxidic nanoparticles is critical in many cases.

A first regulation of this size may be achieved by adopting the suitable preparation methodology for depositing the transition metal ionic species (TMIS) on the support surface (Fig. 1).

One of the two following main alternatives may be adopted. The first one is the conventional *incipient wetness impregnation* (*IWI*). It involves impregnation of the support with an aqueous solution containing one or more TMIS of the active element to be deposited, followed by drying and air-calcination. A volume of the impregnating solution equal to the pore volume of the support and suitable concentration of TMIS is used. During impregnation the TMIS are transferred inside the pores through capillary forces. Then, these are precipitated/crystallized inside or outside the pores. In any case the deposition takes place,

* Corresponding author at: University of Patras, Department of Chemistry, University Campus, Rio, GR-265 00 Patras, Achaia, Greece.
Tel.: +30 2610997114; fax: +30 2610994796.
E-mail address: alycour@chemistry.upatras.gr (A. Lycourghiotis).

0920-5861/$ – see front matter © 2007 Elsevier B.V. All rights reserved.
doi:10.1016/j.cattod.2007.06.069

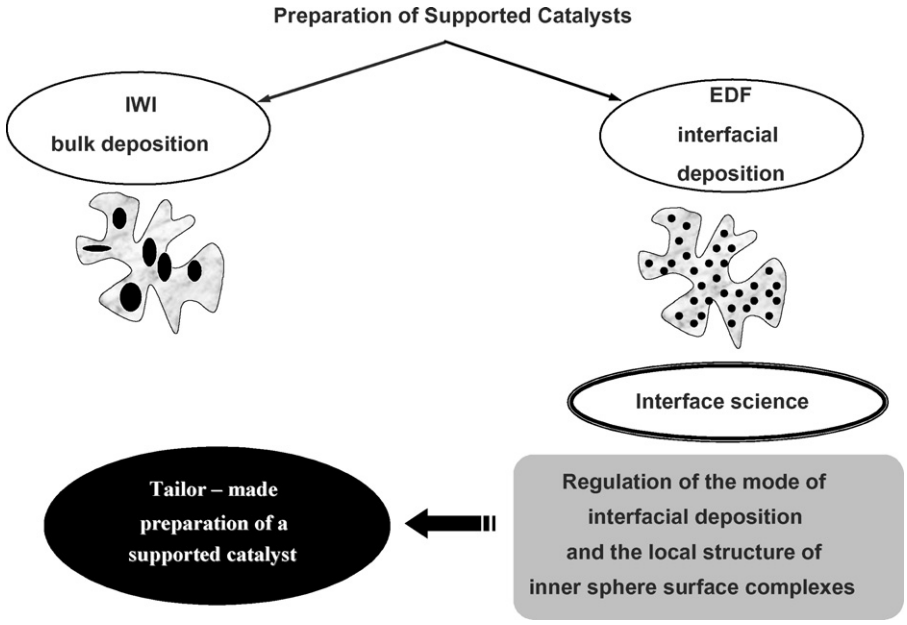

Fig. 1. Optimizing the size of supported oxidic nanoparticles.

mainly, in the bulk solution during drying due to the solvent evaporation. This mode of deposition is defined as *bulk deposition*. The supported particles formed are usually weakly bound on the support surface and transformed *into relatively large supported oxidic particles* during the air-calcination. Therefore, the conventional IWI technique usually leads to catalysts with relatively low active surface and thus relatively low catalytic activity.

The second alternative is the *Equilibrium Deposition Filtration* (*EDF*) technique (Fig. 1). Following this technique the support is immersed in a large volume of a dilute aqueous solution of the TMIS, ideally at fixed pH and ionic strength. Equilibration of the suspension follows for several hours under stirring. During equilibration the TMIS are deposited at the *interface* developed between the support surface and the aqueous solution. This mode of deposition is defined as *interfacial deposition*. In the filtration step the *interfacially* deposited TMIS *are practically* separated from the non-deposited ones. Interfacial deposition results to catalysts with very small supported nanoparticles and thus to very high dispersion of the supported phase [2,3]. This is because their size is controlled by the physicochemical characteristics and the *size of the interface*. The high dispersion and thus the active surface is frequently reflected to the relatively high activity of the final catalysts [2].

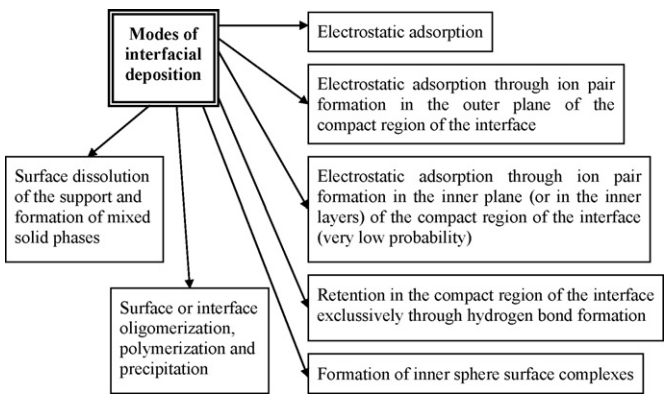

Fig. 2. Modes of interfacial deposition.

A much finer tuning of the size of the supported nanoparticles could be achieved by selecting the mode of interfacial deposition (Fig. 2). This is a complex procedure involving some kind of electrostatic adsorption [4,5], adsorption through hydrogen bonds [6], formation of inner sphere surface complexes [7–9], interfacial polymerization and precipitation [3,10–12] as well as surface dissolution of the support and formation of a mixed phase with the TMIS [13,14] (Fig. 2). It should be noted that the size of the interface depends on the ionic strength of the impregnating solution. It is extended up to 50 Å for low values of the ionic strength [15]. Various models have been developed to describe the interfacial region [12,16,17]. According to the most of these models the interface is divided into two regions, the compact region (extending up to 5 Å from the surface [15]) and the diffuse one.

The relative contribution of each of the aforementioned process to the whole interfacial deposition, for a given support, depends on the nature of the TMIS, the pH and the concentration of the impregnating solution, the ionic strength, the impregnation temperature and the impregnation time. Interface science provides the general strategy and the methodologies for determining the mode of interfacial deposition as well as the local structure of the eventually formed inner sphere complexes, which predominate under given impregnation conditions [18]. This allows the ‘‘selection’’ of the proper mode of interfacial deposition or the local structure mentioned above by adjusting the aforementioned impregnation parameters.

The optimization of the size of the oxidic nanoparticles for two important supported catalysts is the purpose of the present

work. Specifically, we attempted a fine tuning of the size of molybdenum oxide nanoparticles supported on anatase by regulating the local structure of the mononuclear inner sphere surface complexes formed on the support surface. Moreover, we attempted to optimize the size of the ''cobalt oxide'' nanoparticles supported on γ-alumina by regulating the type of deposition (bulk versus interfacial) and the mode of the interfacial deposition (formation of inner sphere complexes versus interface precipitation). Concerning the molybdena catalysts the deposition of the MoO_4^{2-} ions on the support surface was performed using EDF, whereas concerning the ''cobalt oxide'' catalysts both IWI and EDF were used to deposit the $Co(H_2O)_6^{2+}$ aqua complexes on the γ-alumina surface. Most of the experimental results are involved in our previous publications [7,10,11,19–21]. In this work we combine the above results in order to be emerged how the interface science can be used for optimizing the size of oxidic nanoparticles in supported catalysts.

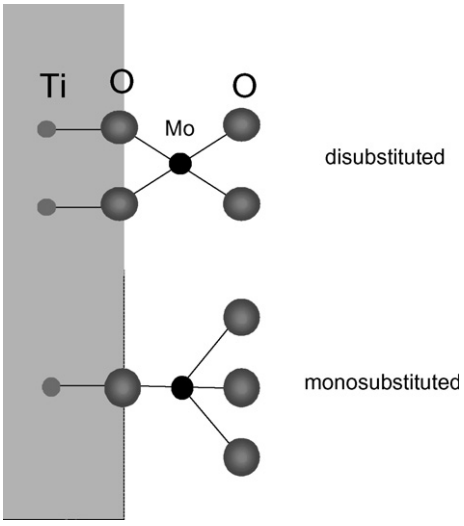

Fig. 3. Adsorption of molybdate monomers on titania (anatase) surface [7].

2. Experimental

Potentiometric titrations, proton–ion titrations, microelectrophoresis, adsorption experiments, DRS and quantitative modeling were used to determine the mode of the interfacial deposition and the local structure. IWI and EDF were used for catalysts preparation. X-ray photoelectron spectroscopy (XPS) and diffuse reflectance spectroscopy (DRS) were used to estimate the size of the supported nanoparticles. The selective catalytic reduction of NO by NH_3 and the complete oxidation of benzene were used as model reactions for the molybdena and ''cobalt oxide'' supported catalysts, respectively. In both cases a fixed bed reactor working under atmospheric pressure has been used for determining the catalytic activity. The experiments done have been presented in previous papers, where full experimental details can be found [7,10,11,19–21].

3. Results and discussion

Molybdenum oxide nanoparticles supported on titania. The interfacial deposition of molybdate monomers (MoO_4^{2-}) and polymers ($Mo_7O_{24}^{6-}$) on the surface of catalytic supports has been the subject of various investigations in the past [22–27,14,28–37] However, only in the case of the Mo deposition on the anatase surface, it had been studied over a wide range of pH and Mo concentration values, using most of the aforementioned techniques and a quantitative modeling based on the Three Plane model and the Charge Distribution principle developed by Hiemstra and coworkers [7]. Concerning the latter, it had been found that the monomeric species are deposited by reacting with the singly coordinated surface hydroxyls of the support, forming monosubstituted and disubstituted inner sphere complexes (Fig. 3). The formation of these species occurs over the entire pH and concentration range studied. However, it had been found that the relative surface concentration of the above inner sphere complexes is pH dependent. At high pH values (e.g. pH 9) the monosubstituted structure is favored versus the disubstituted one. The latter becomes more significant at lower pH values (e.g. pH 6). At high Mo concentrations and pH values lower than 5.5 the polyanion $Mo_7O_{24}^{6-}$ is additionally adsorbed on the anatase surface via electrostatic forces and hydrogen bonds formation.

In order to show the close relation between the local structure and the size of the supported MoO_3 oxidic nanoparticles, we selected two MoO_3/anatase catalysts which had been prepared and characterized by us in another work [19]. These were prepared by EDF at pH 9.1 and pH 6.0 using impregnating solutions containing 1.8×10^{-2} and 1.0×10^{-2} mol Mo dm^{-3}, respectively. After drying and calcination (500 °C for 5 h) the catalysts, with almost the same Mo loading (1.5% wt. MoO_3) were characterized and tested. The disubstituted inner sphere complex is stronger bound on the titania surface than the monosubstituted one. Therefore, the former is expected to resist more effectively to the sintering taking place during calcination, where the inner-sphere complexes are progressively transformed into supported MoO_3 nanoparticles. Thus, smaller MoO_3 supported nanoparticles stronger interacting with the support surface are expected to be obtained for the catalyst prepared at pH 6.0 as they compared to those obtained for the catalyst prepared at pH 9.1. Concerning the size, the above predictions are confirmed by the values of the surface atomic ratio Mo/(Mo + Ti + O) determined by XPS. In fact, this ratio was found to be equal to 2.195 and 1.298 for the catalysts prepared at pH 6 and 9.1, respectively. Concerning the ''support/supported particles'' interactions these predictions are also confirmed by the $F(R\infty)$ values determined at ~380 nm, which estimate these interactions [19]. The DR spectra illustrated in Fig. 4 show, in effect, that these interactions are stronger in the catalyst prepared at pH 6.

It would be now interesting to investigate which one of the aforementioned physicochemical characteristics of the final catalysts related with the size of the supported nanoparticles (active surface, interactions exerted between the support surface and the supported nanoparticles) determines mainly the catalytic activity with respect to the model reaction. Fig. 5 illustrates the values, which had been determined at three

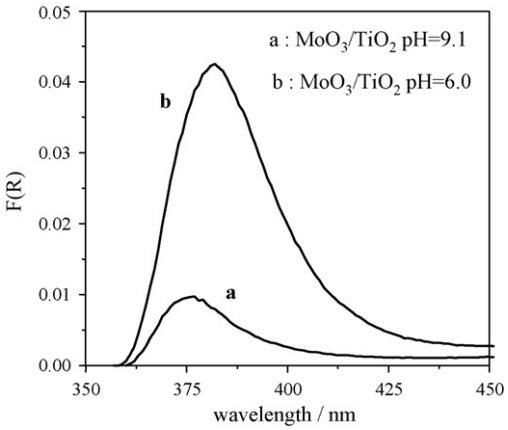

Fig. 4. Diffuse reflectance spectra recorded after calcination, for the molybdena/titania EDF samples prepared at pH 9.1 (a) and 6 (b) [19].

temperatures, for the ratio of the NO conversion obtained over the catalyst prepared at pH 6.0 to that obtained over the catalyst prepared at pH 9.1.

It may be seen that in all temperatures the catalyst prepared at pH 6.0 is more active than the catalyst prepared at pH 9.1 indicating that it is the magnitude of the active phase which mainly determines catalytic activity. These clearly show that the regulation of the local structure of the inner-sphere complexes formed by changing the impregnation conditions may result to supported catalysts with the optimum surface characteristics and thus high activity.

Cobalt oxide nanoparticles supported on γ-alumina. As already mentioned a first optimization of the size of the ''cobalt oxide'' supported nanoparticles is attempted by selecting the type of deposition. Two supported catalysts, both containing 21% Co (w/w) which had been prepared and characterized by us [3], were selected for the present article; the one by IWI and the other one by EDF at pH 7 and Co initial concentration equal to 2.5×10^{-2} mol Co dm^{-3}. The DR spectrum recorded after drying for the IWI specimen is illustrated in Fig. 6.

The main adsorption band at about 530 nm indicates the precipitation of the $Co(H_2O)_6^{2+} \cdot 2NO_3^-$ supported nanoparticles where the Co is in octahedral symmetry [3,11]. The

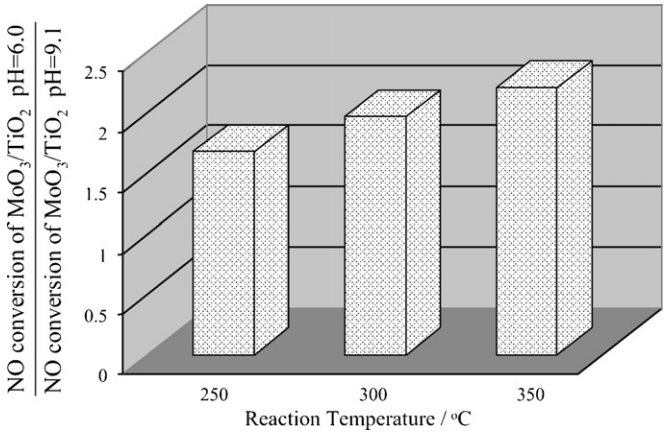

Fig. 5. Values of the ratio of the NO conversion obtained over the catalyst prepared at pH 6.0 to that obtained over the catalyst prepared at pH 9.1 [19].

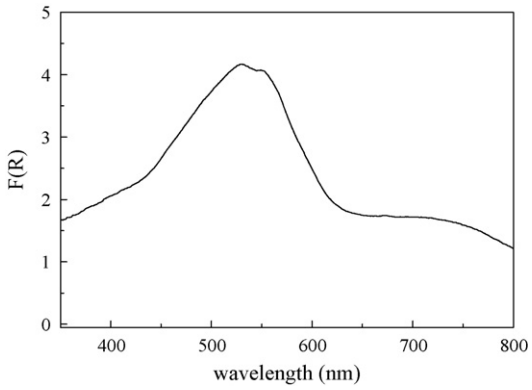

Fig. 6. Diffuse reflectance spectrum recorded after drying for the ''cobalt oxide''/γ-alumina IWI sample [3].

shoulder at about 670 nm indicates that these, presumably loosely bound, nanoparticles are partially transformed into relatively large supported Co_3O_4 nanoparticles even before calcination. The picture changes drastically by imposing interfacial deposition using EDF. The DR spectrum recorded after filtration and before drying for the EDF specimen (Fig. 7) illustrates a DR band centered at about 530 nm and extended to higher wavelengths with a quite clear shoulder centered at about 620 nm. This reflects the presence of the interfacially deposited $Co(H_2O)_6^{2+}$ aqua complex and may be deconvoluted into five peaks [11].

It has been well documented that the peak at about 580 nm reflects the formation of the coordinative Co–O–Al surface bonds by exchanging one or two water ligands with surface oxygens, whereas the peak at about 620 nm the formation of the coordinative Co–O(H)–Co ''lateral'' bonds brought about by condensation between the interfacially deposited $Co(H_2O)_6^{2+}$ ions [11]. The formation of the three-dimensional surface precipitate (Fig. 7) under the impregnating conditions used to prepare this sample has been well documented mainly by spectroscopic, kinetic and proton–ion titration results [10,11,21]. The size of the surface precipitate, mainly along a direction perpendicular to the surface, is relatively small because it is determined by the size and the physicochemical parameters of the interface. This induces the development of quite strong ''supported phase – support'' interactions which hinder its transformation to supported ''cobalt oxide'' nanoparticles during drying and justifies the no detection of a band at about 670 nm in the DR spectrum recorded after drying (not presented here). Moreover, the relatively small size mentioned above is expected to conduct the formation, after calcination, of supported ''cobalt oxide'' nanoparticles with relatively small size compared to the corresponding one of the ''cobalt oxide'' nanoparticles formed after calcination of the IWI sample. The determination of the surface atomic ratio Co/(Co + Al + O) by XPS, which is inversely proportional to the aforementioned size, confirmed this prediction. In fact, this ratio is equal to 2 and 20 for the IWI and the EDF sample, respectively [3]. The relatively high active surface, achieved by selecting the EDF technique and thus imposing interfacial deposition instead of bulk one (Fig. 1) resulted to the preparation of a ''cobalt oxide''/γ-alumina catalyst with

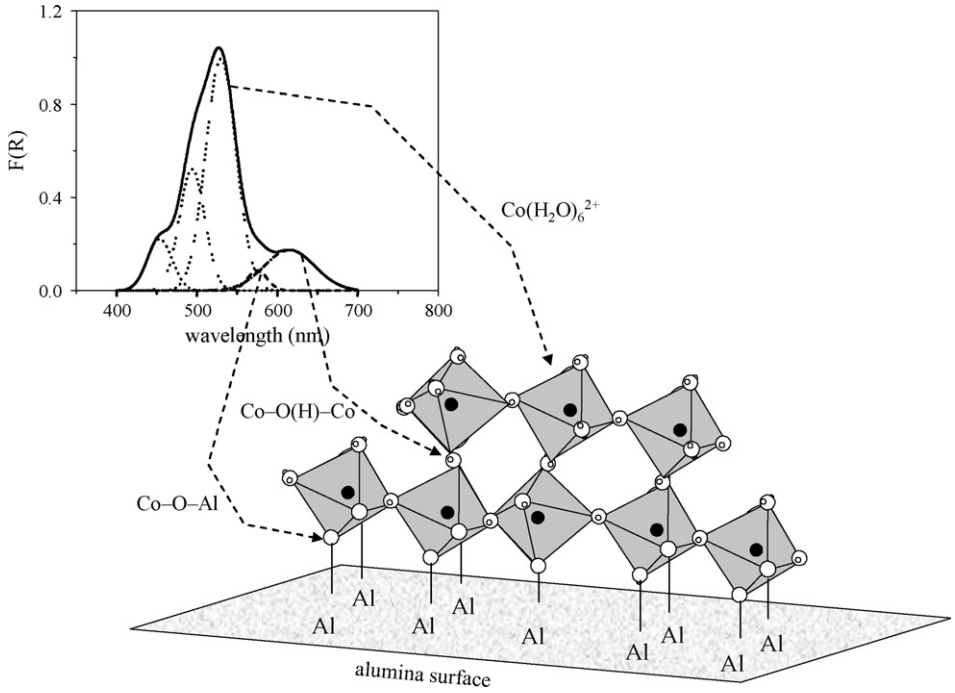

Fig. 7. Diffuse reflectance spectrum recorded after filtration and before drying for the ‘‘cobalt oxide’’/γ-alumina EDF sample and schematic representation of the deposited state.

relatively high activity for the complete oxidation of benzene. In fact, inspection of Fig. 8 clearly shows that the conversion of benzene determined at medium temperatures over the EDF catalyst is considerably higher than that obtained over the IWI catalyst.

A finer tuning of the size of the ‘‘cobalt oxide’’ supported nanoparticles is attempted by selecting the mode of interfacial deposition (namely by selecting, alternatively, the formation of multinuclear inner sphere surface complexes or the formation of three-dimensional surface precipitate (Fig. 2)). Two supported catalysts, both containing 16% Co (w/w), which had been prepared and characterized by us [20], were selected for this article. These had been prepared following EDF. In both cases the deposition took place at pH 7. The determination of the mode of interfacial deposition, using most of the methodologies mentioned in the experimental part, had shown

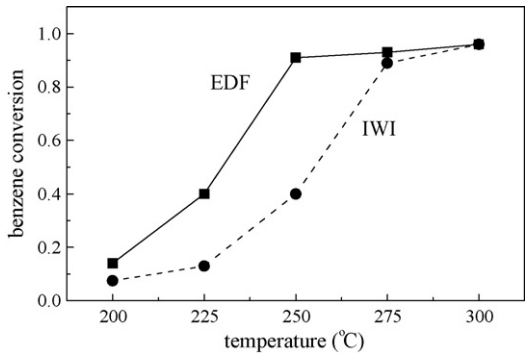

Fig. 8. Values of conversion of benzene determined at various temperatures over two ‘‘cobalt oxide’’/γ-alumina catalysts prepared by EDF and IWI, both containing 21% (w/w) Co [3].

that the formation of the multi nuclear inner sphere surface complexes is favored by performing the deposition in an impregnation solution with Co initial concentration equal to 1.0×10^{-2} mol Co dm^{-3} and adopting an impregnation time equal to 336 h. The sample prepared under these conditions is denoted as EDF-A. In contrast, it had been found that the formation of three-dimensional surface precipitate is favored for Co initial concentration equal to 2.5×10^{-2} mol Co dm^{-3} and impregnation time equal to 96 h. The sample prepared under these conditions is denoted as EDF-B. Fig. 9 illustrates the diffuse reflectance spectra of these samples and the corresponding schematic representations for the deposited states.

Inspection of the spectra clearly shows, in agreement with the above, that the relative magnitude of the deconvolution band at about 620 nm, attributed to the coordinative Co–O(H)–Co bonds [11], is significantly larger in the sample EDF-B. In fact, the ratio of the value of the Kubelka–Munk function determined at 620 nm to that determined at 580 nm was calculated to be equal to 2.2 and 3.1 for the EDF-A and EDF-B sample, respectively. It is obvious that the supported phase in the sample EDF-A is more strongly interacted with the support than that in the sample EDF-B. It is, therefore, expected that the former will be transformed into slightly smaller supported ‘‘cobalt oxide’’ nanocrystallites than the latter. This is confirmed by the XPS measurements, which had performed in the calcined samples. In fact, the value of the surface atomic ratio Co/(Co + Al + O) was found to be equal to 20 and 17 for the sample EDF-A and EDF-B, respectively.

In view of the above it will be interesting to investigate which one of the aforementioned interfacial deposition modes

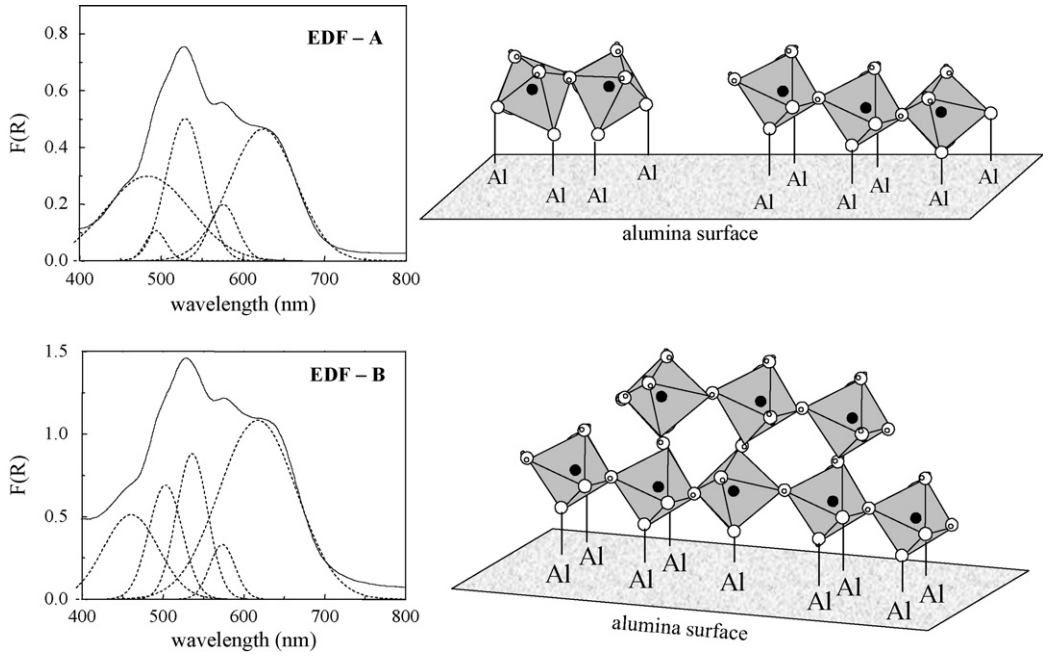

Fig. 9. Diffuse reflectance spectra recorded after filtration and before drying, for the samples EDF-A and EDF-B and the corresponding schematic representations for the deposited states.

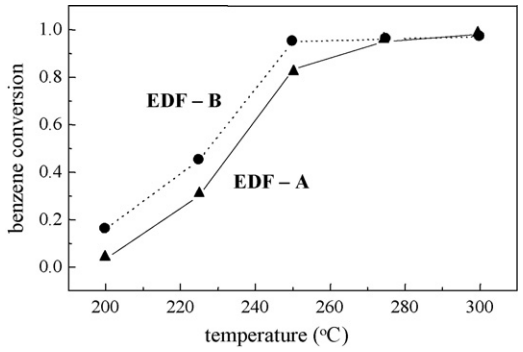

Fig. 10. Values of conversion of benzene determined at various temperatures over the samples EDF-A and EDF-B (see text) [20].

conducts the optimum size of the ''cobalt oxide'' supported nanoparticles with respect to the complete oxidation of benzene.

Inspection of Fig. 10 clearly shows that the values of conversion determined at temperatures lower than 270 °C over the EDF-B catalyst are considerably higher than the corresponding ones obtained over the EDF-A catalyst. This could be attributed to the quite strong interactions exerted between the ''cobalt oxide'' supported nanoparticles and the support in the EDF-A sample. These interactions, quite expectable due to nature of the precursor adsorbed state (multinuclear, two-dimensional inner sphere complexes), may somewhat hinder the exchange of electrons with the adsorbed reactant explaining the relatively low catalytic activity. From the above it may be concluded that the interfacial precipitation leads to the supported ''cobalt oxide''/γ-alumina catalysts with the optimum size of the supported nanoparticles for the complete oxidation of benzene.

4. Conclusions

The following conclusions can be drawn from the present study:

1. An optimization of the size of the supported ''molybdenum oxide''/titania and ''cobalt oxide''/γ-alumina nanoparticles may be achieved by ''selecting'', respectively, the local structure and the proper mode of deposition related to the first, critical, step of catalyst preparation.
2. Concerning the ''molybdenum oxide''/titania catalysts it was found that the disubstituted Mo inner sphere surface complexes formed at pH 6, which are bound on the support surface stronger than the monosubstituted ones formed at pH 9, resist more effectively to the sintering taking place during calcination where the above complexes are transformed progressively into MoO_3 supported nanoparticles. This leads to a catalyst with very small MoO_3 nanoparticles and thus with very high activity for the selective reduction of NO by NH_3.
3. Concerning the ''cobalt oxide''/γ-alumina catalysts it was found that a relatively large (small) size of the supported nanocrystallites is imposed by the bulk deposition (formation of inner sphere surface complexes). A quite small size of the supported ''cobalt oxide'' nanocrystallites not strongly interacted with the support surface is imposed by the interface precipitation. This is the optimum supported phase for the complete oxidation of benzene.

References

[1] A.T. Bell, Science 299 (2003) 1688.
[2] A. Lycourghiotis, Ch. Kordulis, K. Bourikas, Encyclopedia of Surface and Colloid Science, Marcel Dekker, Inc., 2002,, p. 1366.

[3] T. Ataloglou, J. Vakros, K. Bourikas, Ch. Fountzoula, Ch. Kordulis, A. Lycourghiotis, Appl. Catal. B 57 (2004) 299.
[4] C. Park, P.A. Fenter, N.C. Sturchio, J.R. Regalbuto, Phys. Rev. Lett. 94 (2005), 076104/1.
[5] M. Schreier, J.R. Regalbuto, J. Catal. 225 (2004) 190.
[6] J.R. Bargar, S.N. Towle, G.E. Brown Jr., G.A. Parks, J. Colloid Interface Sci. 185 (1997) 473.
[7] K. Bourikas, T. Hiemstra, W.H. Van Riemsdijk, J. Phys. Chem. B 105 (2001) 2393.
[8] C.J. Chisholm-Brawse, P.A. O'Day, G.E. Brown Jr., G.A. Parks, Nature 348 (1990) 528.
[9] S. Boujday, J.-F. Lambert, M. Che, Chem. Phys. Chem. 5 (2004) 1003.
[10] T. Ataloglou, K. Bourikas, J. Vakros, Ch. Kordulis, A. Lycourghiotis, J. Phys. Chem. B 109 (2005) 4599.
[11] J. Vakros, K. Bourikas, S. Perlepes, Ch. Kordulis, A. Lycourghiotis, Langmuir 20 (2004) 10542.
[12] K. Bourikas, Ch. Kordulis, J. Vakros, A. Lycourghiotis, Adv. Colloid Interface Sci. 110 (2004) 97.
[13] X. Carrier, J.-B. d'E, de la Caillerie, J.-F. Lambert, M. Che, J. Am. Chem. Soc. 121 (1999) 3377.
[14] X. Carrier, J.-F. Lambert, M. Che, J. Am. Chem. Soc. 119 (1997) 10137.
[15] T. Hiemstra, W.H. Van Riemsdijk, J.Colloid Interface Sci. 179 (1996) 488.
[16] J. Lyklema, Fundamentals of interface and colloid science, Solid–Liquid Interfaces, 2, Academic Press, London, 1995.
[17] W. Stumm, Chemistry of the Solid–Water Interface, Wiley, New York, 1992.
[18] K. Bourikas, G.D. Panagiotou, Th. Petsi, Ch. Kordulis, A. Lycourghiotis, Stud. Surf. Sci. Catal. 162 (2006) 251.
[19] Ch. Fountzoula, N. Spanos, H.K. Matralis, Ch. Kordulis, Appl. Catal. B 35 (2002) 295.
[20] T. Ataloglou, Ch. Fountzoula, K. Bourikas, J. Vakros, A. Lycourghiotis, Ch. Kordulis, Appl. Catal. A 288 (2005) 1.
[21] J. Vakros, K. Bourikas, Ch.A. Kordulis, Lycourghiotis, in: Proceedings of the Europacat VII, Sofia, Bulgaria, August 28–September 01, 2005.
[22] N. Spanos, L. Vordonis, Ch. Kordulis, A. Lycourghiotis, J. Catal. 124 (1990) 301.
[23] N. Spanos, L. Vordonis, Ch. Kordulis, P.G. Koutsoukos, A. Lycourghiotis, J. Catal. 124 (1990) 315.
[24] N. Spanos, A. Lycourghiotis, J. Catal. 147 (1994) 57.
[25] N. Spanos, H.K. Matralis, Ch. Kordulis, A. Lycourghiotis, J. Catal. 136 (1992) 432.
[26] K. Bourikas, N. Spanos, A. Lycourghiotis, J. Colloid Interface Sci. 184 (1996) 301.
[27] K. Bourikas, M.A. Goula, A. Lycourghiotis, Langmuir 14 (1998) 4819.
[28] C. Louis, M. Che, J. Catal. 135 (1992) 156.
[29] M.J. Vissenberg, L.J.M. Joosten, M.M.E.H. Heffels, A.J. van Welsenes, V.H.J. de Beer, R.A. van Santen, J.A.R. van Veen, J. Phys. Chem. B 104 (2000) 8456.
[30] D.S. Kim, I.E. Wachs, K. Segawa, J. Catal. 149 (1994) 268.
[31] S.D. Kohler, J.G. Ekerdt, D.S. Kim, I.E. Wachs, Catal. Lett. 16 (1992) 231.
[32] J.A. Bergwerff, T. Visser, B.R.G. Leliveld, B.D. Rossenaar, K.P. de Jong, B.M. Weckhuysen, J. Am. Chem. Soc. 126 (2004) 14548.
[33] J.A.R. Van Veen, P.A.J.M. Hendriks, E.J.G.M. Romers, R.R. Andrea, J. Phys. Chem. 94 (1990) 5275.
[34] J.A.R. Van Veen, P.A.J.M. Hendriks, R.R. Andrea, E.J.G.M. Romers, A.E. Wilson, J. Phys. Chem. 94 (1990) 5282.
[35] C.T.J. Mensch, J.A.R. Van Veen, B. Van Wingerden, M.P. Van Dijk, J. Phys. Chem. 92 (1988) 4961.
[36] J.A.R. Van Veen, H. De Wit, C.A. Emeis, P.A.J.M. Hendriks, J. Catal. 107 (1987) 579.
[37] J.A.R. Van Veen, P.A.J.M. Hendriks, Polyhedron 5 (1986) 75.